Photogrammetrically Determined Cloud-Free Lines-Of-Sight Through The Atmosphere

IVER A. LUND

Air Force Cambridge Research Laboratories, Bedford, Mass. 01730

AND MILTON D. SHANKLIN

University of Missouri, Columbia 65201

(Manuscript received 28 January 1972, in revised form 17 March 1972)

ABSTRACT

Relative frequencies of cloud-free lines-of-sight were determined at specified elevation angles and directions by utilizing data from photographs taken with a camera with a 180° (fish-eye) lens and infrared film to produce high-quality photographs of the sky. Four summers of hourly daytime data were used to find relative frequencies as functions of viewing angle, sky cover, sunshine and cloud type. Persistence and recurrence relative frequencies, comparisons between "clear" and cloud-free lines-of-sight, and a general method for estimating probabilities of cloud-free lines-of-sight for any location are presented and discussed.

1. Introduction

Estimates of the probability of cloud-free lines-of-sight are required for such purposes as determining the utility of optical and infrared search and tracking systems, judging the operational value of devices which require bright sunshine, or moonlight, and approximating insolation at the surface of the earth. Methods for estimating the required probabilities from available meteorological observations have been developed by Blackmer and Harllee (1960), Fox (1961), Appleman (1962), McCabe (1965), Lund (1965, 1966), Brintzenhofe *et al.* (1971) and others, but none of these methods are entirely satisfactory. Methods based on weather observers' estimates of sky cover often do not take into account the angle of view through the atmosphere, or the fact that observers see the sides of clouds as well as their bases when they estimate sky cover, tending to overestimate total earth cover. Methods based on sunshine observations do not yield accurate probabilities of cloud-free lines-of-sight since the sunshine recorder does not detect "thin" clouds. Cloud photographs taken from satellites lack the resolution required to obtain precise probabilities.

Bertoni (1967) described a program for obtaining, directly, seeing conditions on a family of lines-of-sight. The observations are taken by observers while in flight, thus having the added advantage of providing probabilities for lines to and from various altitudes. Most other methods are limited to lines to and from the surface of the earth and space. Observations taken by observers while in flight may be the most precise, but observers experience difficulty in distinguishing between haze and thin clouds, and there is difficulty in obtaining sufficient inflight observations to prepare reliable estimates of the climatic probabilities.

By utilizing a camera with a 180° (fish-eye) lens and infrared film, high contrast photographs of the whole sky were taken from the U. S. National Weather Service observing site at Columbia, Mo. Photographs cover every daylight hour for a period of more than three years. Studies based on these observations are described by Pochop and Shanklin (1966), Bundy (1969), and Shanklin and Landwehr (1971).

Only observations taken during June through August from 1966 through 1969 are discussed in this paper. More hourly daylight observations were available for summer than any other season, thus permitting studies of hourly persistence and recurrence probabilities to extend over longer time periods.

Relative frequencies of cloud-free lines-of-sight as functions of viewing angle, sky cover, sunshine and cloud type are presented. Comparisons between "clear" and cloud-free lines-of-sight are made and a general method for estimating probabilities for other locations is discussed.

2. Determination of cloud-free lines-of-sight

a. Equipment

A Nikon Model F (35 mm) camera with a 180° (fish-eye) lens was used to photograph the whole sky. The 180° lens was chosen instead of a regular lens/spherical mirror combination because of its compactness and simplicity. One of the problems associated with wide-angle lenses, however, is the relationship between the image position on the negative and the

y	θ°	Δθ
0.5	3.58	
1.0	7.17	3.59
1.5	10.76	3.59
2	14.35	3.59
2.5	17.96	3.61
3	21.57	3.61
3.5	25.21	3.64
4	28.86	3.65
4.5	32.52	3.66
5	36.21	3.69
5.5	39.92	3.71
6	43.65	3.73
6.5	47.40	3.75
7	51.18	3.78
7.5	54.96	3.78
8	58.79	3.83
8.5	62.58	3.79
9	66.41	3.83
9.5	70.23	3.82
10.0	74.10	3.87
10.5	77.94	3.84
11.0	81.75	3.81
11.5	85.50	3.75
12.0	89.21	3.71

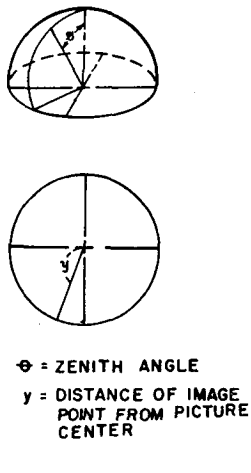

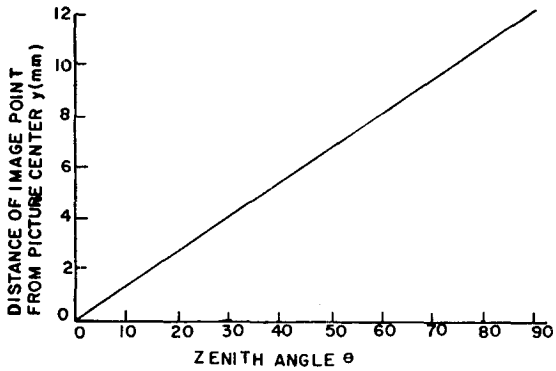

FIG. 1. Relationship between zenith angle and distance of image point from picture center (Ehrenreich Photo Optical Industries, 1965).

object position in space; however, with the lens selected, the relation of the zenith angle to distance of the image point from the center of the picture is nearly linear as shown in Fig. 1, and by Ehrenreich Photo Optical Industries (1965). Thus, the location of the lines-of-sight at the equally incremented elevation angles is easily defined on the negatives as equally incremented distances from the edge of the picture to the center.

The lens specifications include a focal length of 8 mm, an aperture scale of F:8 to F:22, a fixed focus, and six self-contained filters.

In order to extend the range of the camera beyond the ability of the human eye to detect clouds, Kodak Infrared IR 135 film, exposed through a Wratten No. 25 filter, was used. Infrared film is sensitive to the far red and infrared [to approximately the 0.84 μ (Eastman Kodak, 1959) region of the spectrum] as well as the blue region; however, the red filter absorbs the blue sky light so that the film sees clouds not visible to the human eye and shows high contrast between sky and visible clouds.

The lens was shielded from direct sunlight by a rotating sunshield 127 mm in diameter attached to a rod parallel to the motor shaft of an equatorial mount making one revolution per day. Thus, the sunshield followed the sun across the sky keeping the lens shaded to prevent direct sunlight from entering the lens. A seasonal adjustment of the length of the rod was necessary to allow for the change of the elevation angle of the sun and, at the same time, the change in the length of the day.

The camera was operated by remote control in conjunction with a Nikon motor drive Model F-36 in place of the regular camera back permitting 36 exposures per film load. An electric timer controlled the sequential operation of the camera and a dc power supply provided the power for the motor drive of the camera.

For weather protection, the camera was placed inside a 24-cm diameter glass dome optically ground and polished on both surfaces. The temperature inside the dome was moderated using forced ventilation with filtered air and thermostatically controlled heat lamps.

The photographic equipment was located on the roof of the National Weather Service Building at the Columbia Municipal Airport. A picture of the camera setup is shown in Fig. 2.

b. Data collection procedure

Hourly exposures were made at 5 min before the hour concurrent with the National Weather Service observations between sunrise and sunset during the periods 1 March 1966 to 28 February 1969 and 1 June 1969 to 31 August 1969. As mentioned in the Introduction only the June through August data were used in this study. The camera was set for an exposure time

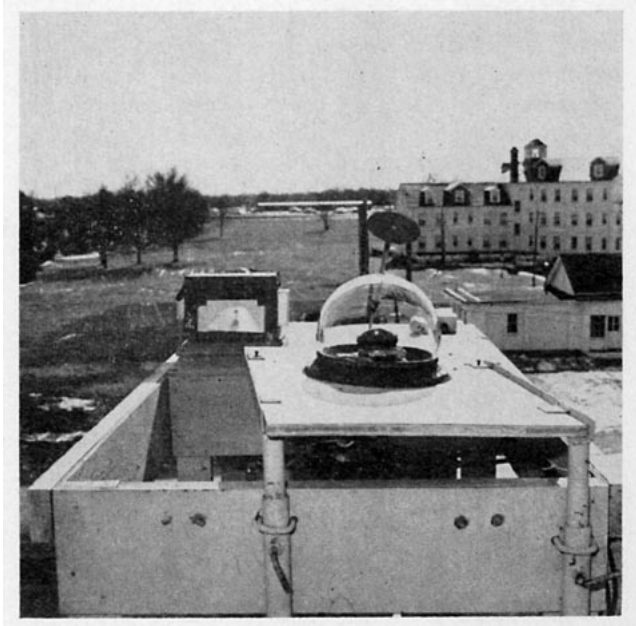

FIG. 2. An overall view of the Nikon F camera, sunshield, and glass dome (Bundy, 1969).

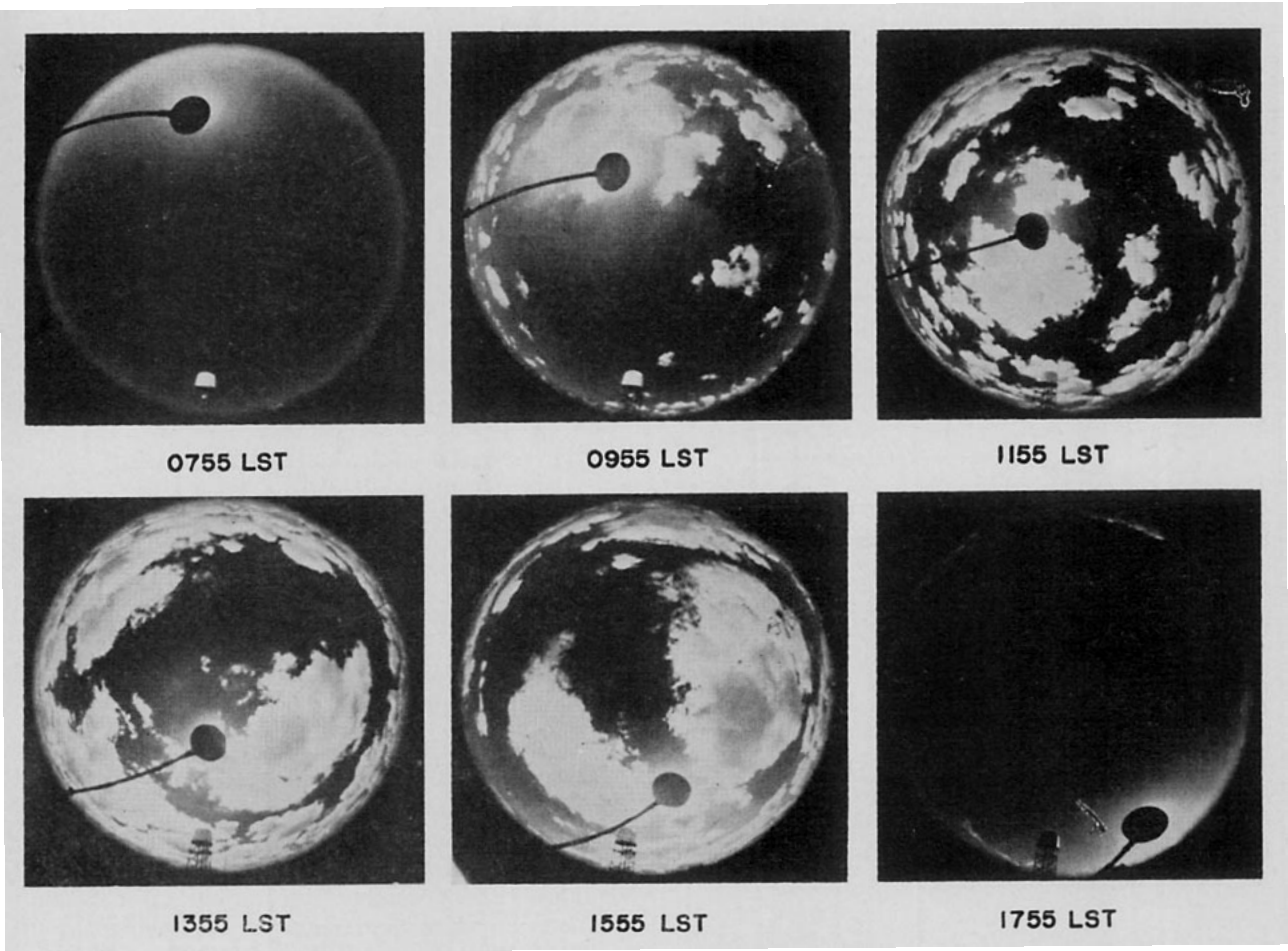

FIG. 3. An example of one day's photographs of the whole sky (Bundy, 1969). Photographs were taken every daylight hour but only one-half of them are shown to conserve space.

of $\frac{1}{8}$ sec and an aperature of F:8. The number of daily exposures varied from eleven in winter to fourteen in summer. An example of one day's photographs is shown in Fig. 3. Photographs were taken every daylight hour but only one-half of them are shown to conserve space.

The film was changed every second day and a log kept to identify the day and hour of every exposure. The film was developed with Diafine, a two-bath developer, and the negatives were printed on 8×10 inch Dupont Varilour R paper using a No. 4 Varilour filter to insure maximum contrast. The picture size was 19 cm, an enlargement of approximately eight times.

In order to locate the exact positions of the lines-of-sight on the prints, a clear plastic template (Fig. 4), 19 cm in diameter, the exact size of the photographs, was placed over the photographs. The elevation angles were measured along the radii. By observing Polaris with a transit placed over the camera lens and taking sidereal time into effect, true north was determined and the true azimuth of a nearby anemometer stand, clearly visible on all photographs, was determined. Thus, the template and the photographs were oriented by placing the azimuth of the anemometer stand on the template over the image of the stand on the photograph.

The superimposed template contained 33 small circles whose centers represent the 33 lines-of-sight at azimuths of 0°, 90°, 180° and 270° and elevation angles

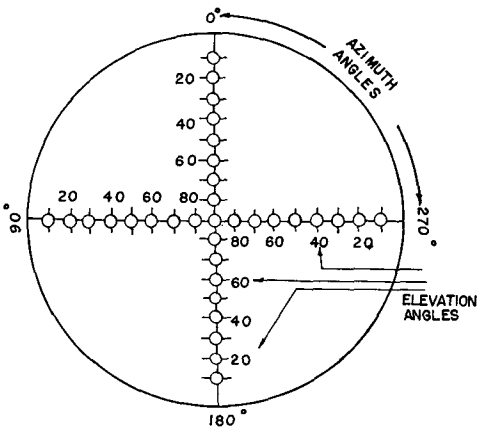

FIG. 4. Template used to determine azimuth and elevation angles (Bundy, 1969).

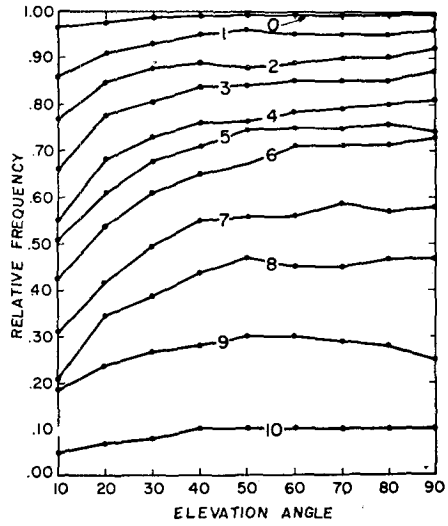

FIG. 5. Relative frequency of a cloud-free line-of-sight as a function of elevation angle and National Weather Service observed total sky cover, in tenths (without smoothing).

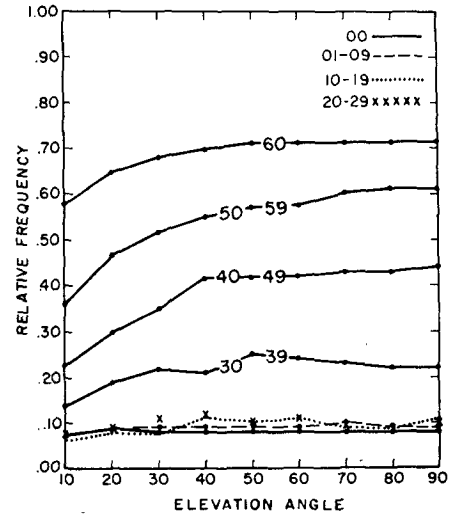

FIG. 6. Relative frequency of a cloud-free line-of-sight as a function of elevation angle and National Weather Service observed sunshine duration, in minutes.

of 10° to 90° in increments of 10°. Each line-of-sight was examined for the presence of clouds and each point was double-checked to reduce errors. Prints were not prepared of negatives that showed either no clouds or completely overcast skies; in these cases all 33 lines-of-sight were concluded to be, respectively, either all clear or all cloudy.

3. Determination of cloudiness and sunshine

Routine National Weather Service (NWS) cloudiness and sunshine observations at Columbia were used in this study. They were taken from the same site and at the same time as the photographs. Hourly observations of total sky cover and total opaque sky cover, minutes of sunshine recorded each hour, and three-hourly cloud types were studied to determine relationships between these parameters and cloud-free lines-of-sight as determined from the photographs.

4. Observed relative frequencies of cloud-free lines-of-sight

Although relative frequencies of cloud-free lines-of-sight over Columbia are of some interest, the primary purpose of this study was to develop a general method for estimating probabilities of cloud-free lines-of-sight between the surface of the earth and space from conventional surface weather observations taken at any location. In order to develop such a method, data extracted from photographs were related to NWS observations of sky cover, sunshine and cloud types, taken from the same site at the same time. The following subsections describe how these parameters are related to probabilities of cloud-free lines-of-sight.

a. As a function of sky cover

The relative frequency (an estimate of the probability) of a cloud-free line-of-sight was found for each elevation angle as a function of the tenths of cloudiness

TABLE 1. Relative frequencies of cloud-free lines-of-sight as a function of elevation angle and National Weather Service observed total sky cover. Observations were taken hourly at Columbia, Mo., June through August from 1966 through 1969.

Total sky cover (tenths)	Elevation angle 10°	20°	30°	40°	50°	60°	70°	80°	90°	Sample size	Relative frequency
0	0.97	0.98	0.99	0.99	0.99	0.99	0.99	0.99	0.99	2044	0.153
1	0.86	0.91	0.93	0.95	0.96	0.95	0.95	0.95	0.96	832	0.062
2	0.77	0.85	0.88	0.89	0.88	0.89	0.90	0.90	0.92	900	0.067
3	0.66	0.78	0.81	0.84	0.84	0.85	0.85	0.85	0.87	876	0.066
4	0.55	0.68	0.73	0.76	0.76	0.78	0.79	0.80	0.81	700	0.052
5	0.51	0.61	0.68	0.71	0.75	0.75	0.75	0.76	0.74	588	0.044
6	0.42	0.54	0.61	0.65	0.67	0.71	0.71	0.71	0.73	848	0.064
7	0.31	0.42	0.50	0.55	0.56	0.56	0.59	0.57	0.58	916	0.069
8	0.21	0.35	0.39	0.44	0.47	0.45	0.45	0.47	0.47	1104	0.083
9	0.19	0.24	0.27	0.28	0.30	0.30	0.29	0.28	0.25	1008	0.076
10	0.05	0.07	0.08	0.10	0.10	0.10	0.10	0.10	0.10	3532	0.265
Average (5.67)	0.44	0.51	0.54	0.56	0.56	0.57	0.57	0.57	0.57	13,348	

TABLE 2. Relative frequencies of cloud-free lines-of-sight as a function of elevation angle and National Weather Service observed total opaque sky cover.

Total opaque sky cover (tenths)	Elevation angle 10°	20°	30°	40°	50°	60°	70°	80°	90°	Sample size	Relative frequency
0	0.92	0.95	0.96	0.96	0.97	0.97	0.97	0.97	0.97	2800	0.210
1	0.71	0.81	0.84	0.86	0.88	0.89	0.89	0.88	0.88	1212	0.091
2	0.58	0.68	0.74	0.78	0.77	0.80	0.79	0.80	0.82	1216	0.091
3	0.47	0.58	0.64	0.67	0.69	0.69	0.70	0.70	0.71	1348	0.101
4	0.35	0.45	0.50	0.56	0.56	0.55	0.56	0.56	0.57	988	0.074
5	0.34	0.44	0.50	0.52	0.56	0.57	0.57	0.57	0.55	708	0.053
6	0.23	0.33	0.39	0.40	0.45	0.45	0.45	0.46	0.48	932	0.070
7	0.18	0.28	0.29	0.34	0.35	0.34	0.36	0.38	0.37	696	0.052
8	0.11	0.18	0.18	0.23	0.23	0.24	0.21	0.19	0.20	628	0.047
9	0.12	0.13	0.13	0.13	0.14	0.14	0.14	0.14	0.13	648	0.049
10	0.03	0.04	0.04	0.04	0.04	0.04	0.04	0.04	0.04	2172	0.163
Average (4.36)	0.44	0.51	0.54	0.56	0.56	0.57	0.57	0.57	0.57	13,348	

reported by the NWS. For example, there were in the sample 175 hours when the NWS reported 0.4 total sky cover. The data extracted from the concurrent 175 photographs showed that the lines-of-sight were cloud-free at 10° 55% of the time, at 20° 68% of the time,..., at 80° 80% of the time, and at 90° 81% of the time. This is shown in Table 1, line 5. The sample size is given as 700 instead of 175 since observations, with the exception of 90°, were taken along all four cardinal directions.

Fig. 5 depicts relative frequencies of cloud-free lines-of-sight as a function of elevation angle and NWS observed total sky cover. The curves are shown with no smoothing applied. The relationships between the relative frequencies determined from photographs and sky cover estimated by weather observers are remarkably good. The only departure from what might be expected is the failure of the relative frequencies to always increase as the zenith angle (90°) is approached. This failure is most likely due to the fact that overhead clouds are easier to detect. Table 1 shows the relative frequencies plotted in Fig. 5 and the size of the samples used. A total of 13,348 observations were used to prepare Fig. 5. Table 2 shows relative frequencies as a function of opaque clouds only. These values may be useful for evaluating optical or infrared systems that are capable of observing through thin clouds.

b. As a function of sunshine

Fig. 6 depicts relative frequencies of cloud-free lines-of-sight as a function of elevation angle and minutes of observed sunshine. The values, also shown in Table 3, conform well to expectations. The fact that relative frequencies of cloud-free lines-of-sight never exceed 71% even when sunshine is recorded continually (60 min per hour) illustrates that sunshine recorders record sunshine even in the presence of "thin" clouds and partial cloud cover. It also implies that there are significant differences between clear, as defined by Lund (1966), and cloud-free lines-of-sight, discussed in Section 7.

c. As a function of cloud form and amount

Since cloud types were reported only at 3-hr intervals, the 0900, 1200 and 1500 LST photographs were studied to determine relationships between cloud forms and relative frequencies of cloud-free lines-of-sight. Data extracted from the photographs were divided into the five categories shown in Table 4, depending upon the form of cloud reported. Tables of relative frequencies of cloud-free lines-of-sight as functions of cloud form, cloud amount and elevation angle, were prepared. With the exception of the cumuliform cloud category, the data samples were too small to identify significant

TABLE 3. Relative frequencies of cloud-free lines-of-sight as a function of elevation angle and National Weather Service observed hourly sunshine duration.

Sunshine duration (min)	Elevation angle 10°	20°	30°	40°	50°	60°	70°	80°	90°	Sample size
00	0.08	0.09	0.08	0.08	0.08	0.08	0.08	0.08	0.08	1164
01–09	0.08	0.08	0.09	0.09	0.09	0.09	0.10	0.09	0.09	296
10–19	0.06	0.08	0.08	0.11	0.10	0.11	0.09	0.08	0.11	248
20–29	0.07	0.08	0.11	0.12	0.10	0.11	0.10	0.09	0.10	324
30–39	0.14	0.19	0.22	0.21	0.25	0.24	0.23	0.22	0.22	424
40–49	0.23	0.30	0.35	0.42	0.42	0.42	0.43	0.43	0.44	640
50–59	0.36	0.47	0.52	0.55	0.57	0.58	0.60	0.61	0.62	1668
60	0.58	0.65	0.68	0.70	0.71	0.71	0.71	0.71	0.71	8584

TABLE 4. Cloud type categories.

Category	Cloud type	Form
1	Altocumulus Altocumulus castellanus Altostratus	Middle
2	Cirrocumulus Cirrostratus Cirrus	Cirriform
3	Cumulonimbus Cumulonimbus mammatus Cumulus Fractocumulus	Cumuliform
4	Fractostratus Nimbostratus Stratocumulus Stratus	Stratiform
5	No clouds, mixtures of more than one form, or unknown	

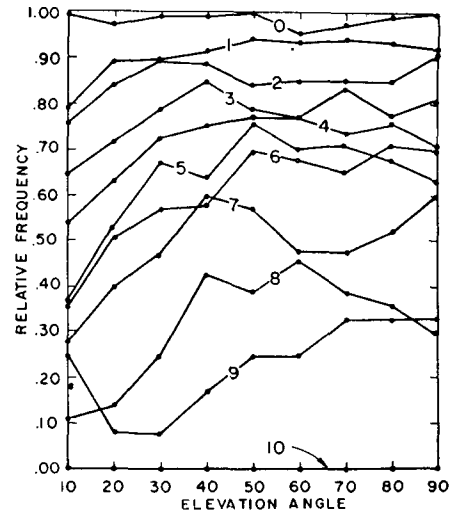

FIG. 7. Relative frequency of a cloud-free line-of-sight as a function of elevation angle and National Weather Service observed total sky cover, in tenths, when one or more of the following cloud types are reported: cumulonimbus, cumulonimbus mammatus, cumulus, fracto-cumulus (cumuliform clouds only) (without smoothing).

departures from the curves shown in Fig. 5. Although the curves shown in Fig. 7, which are based on data observed when cumuliform clouds were the only clouds reported, are irregular, they exhibit a greater tendency for increasing relative frequencies as the zenith angle is approached than is shown in the curves of Fig. 5. This is consistent with expectations since cumulus clouds usually have large vertical dimensions resulting in the sides of the clouds obstructing vision.

5. Persistence

Since photographs were taken hourly, the duration of cloud-free lines-of-sight between photographs is unknown. One might assume that lines-of-sight that are cloud-free in successive photographs are also cloud-free in the intervening time, but this is generally a poor assumption, since cloudiness often varies greatly over short periods of time. *Persistence is defined for this study as an uninterrupted hourly sequence of cloud-free, or cloudy, lines-of-sight.* If the time interval between photographs was 1 min, for example, the decay of persistence might be considerably different. Table 5 and Fig. 8 show, for example, that if there is a cloud-free line-of-sight at an initial time of 0700 LST there is an 83.7% chance that it will be cloud-free at 0800 LST one hour later, a 76.7% chance that it will be cloud-free at both 0800 and 0900 LST,..., and a 26.5% chance that it will be cloud-free at all ten hourly observations following 0700 LST. The heavy line shown in Fig. 8 is the median decay of persistence. The dotted line shows a simple Markov decay, which assumes that the probability of a cloud-free line-of-sight at a given hour is only dependent on the probability for the previous and no other hour. Mathematically, $P(C_1, C_2, \ldots, C_n|C_0)=0.81^n$, where n is the lag in hours.

Fig. 9 depicts the persistence of a cloudy line-of-sight,

TABLE 5. Percent relative frequency of an uninterrupted cloud-free line-of-sight (persistence), given that the line-of-sight was cloud-free at the initial hour. The unconditional relative frequency is the estimated probability of a cloud-free line-of-sight at the initial hour when data for all azimuth and elevation angles are combined.

Initial hour (LST)	Subsequent hour (LST) 0800	0900	1000	1100	1200	1300	1400	1500	1600	1700	Unconditional probability
0700	83.7	76.7	68.0	58.2	48.7	35.2	31.7	29.2	27.7	26.5	58.9
0800		88.6	76.0	63.7	53.2	45.0	34.4	31.6	30.0	27.9	56.2
0900			82.9	68.9	56.6	47.9	40.8	33.6	31.8	28.4	56.5
1000				79.9	65.2	54.2	45.9	40.7	35.5	30.2	54.7
1100					79.1	64.4	53.7	46.9	42.8	33.9	51.5
1200						78.6	64.3	55.6	49.8	47.0	50.0
1300							77.8	64.7	56.8	52.8	52.2
1400								79.5	68.7	63.2	52.9
1500									82.2	74.1	55.3
1600										87.9	57.6
1700											65.5

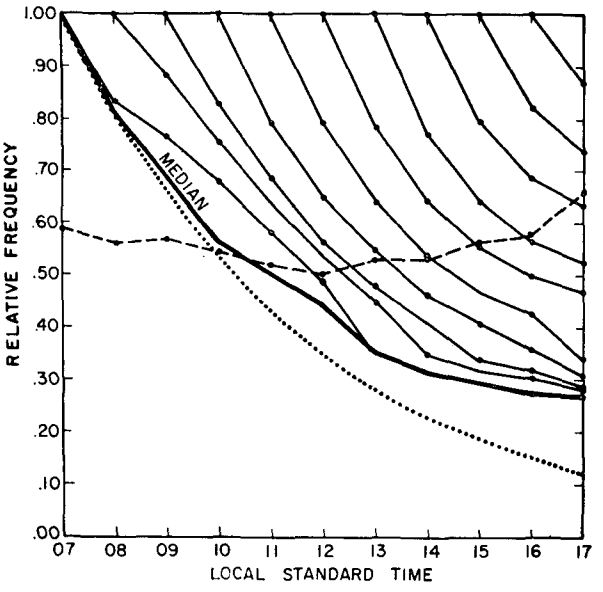

FIG. 8. Relative frequency of an uninterrupted cloud-free line-of-sight (persistence). The dashed line depicts the unconditional relative frequency of a cloud-free line-of-sight, the heavy line the median decay of persistence, and the dotted line a simple Markov decay (P_0^n) when P_0, the hour-to-hour decay, is 0.81 and n is the lag, in hours.

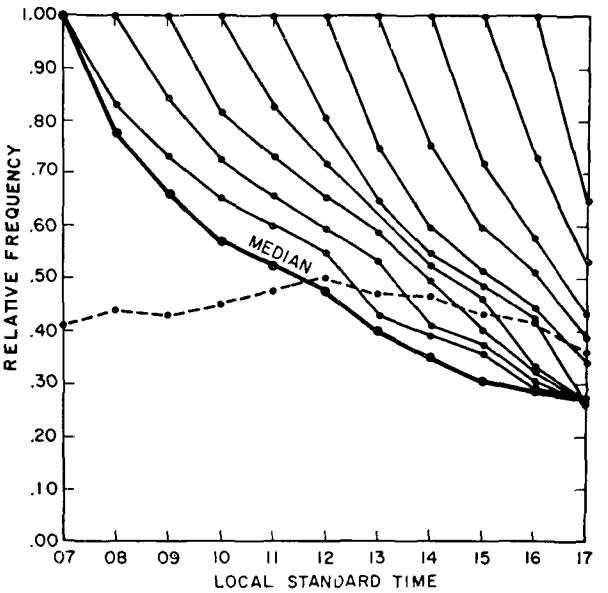

FIG. 9. Relative frequency of an uninterrupted cloudy line-of-sight (persistence). The dashed line depicts the unconditional relative frequency of a cloudy line-of-sight and the heavy line the median decay of persistence.

given that it is cloudy at the initial hour. Data for all azimuth and elevation angles are combined for the study of persistence.

6. Recurrence

Recurrence is defined as the relative frequency (an estimate of conditional probability) of an event recurring at some later hour, given that the event occurred at the initial hour. Table 6 and Fig. 10 show relative frequencies of recurrence of cloud-free lines-of-sight, and Fig. 11 shows relative frequencies of recurrence of cloudy lines-of-sight. The unconditional relative frequencies are also shown in Figs. 10 and 11. Data for all azimuth and elevation angles are combined for the study of recurrence.

An expression for estimating conditional probabilities from the unconditional values, which are more stable since they are based on larger samples of data, has been proposed by McAllister (1969). It is of the form

$$\hat{P}(C_t|C_0)=P(C_t)+[1-P(C_0)]\exp(-at^b), \quad (1)$$

where, in this example, $\hat{P}(C_t|C_0)$ is the estimated probability of observing a cloud-free line-of-sight t hours later, given that it was cloud-free at the initial hour (0), $P(C_t)$ is the unconditional probability of a cloud-free line-of-sight at time t hours later, $P(C_0)$ is the unconditional probability at the initial time, and a and b are constants.

McAllister obtained parameter values of $a=0.263$ and $b=0.632$ for cloud cover data. Gringorten (1971) found a to be a function of the probability of the event and its persistence, and found a best single approximation for b of 0.620. The least-squares best fit to the

TABLE 6. Relative frequency of recurrence of a cloud-free line-of-sight, given that the line-of-sight was cloud-free at the initial hour. The values in parentheses are deviations between the observed relative frequencies and estimated recurrence probabilities (see text).

Initial hour (LST)	Subsequent hour (LST) 0800	0900	1000	1100	1200	1300	1400	1500	1600	1700	Sample size
0700	0.84(0.00)	0.81(0.02)	0.78(0.04)	0.71(0.03)	0.66(0.01)	0.67(0.02)	0.65(0.01)	0.69(0.03)	0.71(0.04)	0.78(0.04)	4395
0800		0.89(0.03)	0.80(0.01)	0.72(0.00)	0.68(0.00)	0.69(0.01)	0.67(0.00)	0.70(0.02)	0.71(0.02)	0.77(0.02)	4192
0900			0.83(−0.01)	0.76(0.00)	0.70(0.00)	0.72(0.02)	0.68(0.00)	0.70(0.01)	0.72(0.02)	0.78(0.02)	4211
1000				0.80(−0.02)	0.73(−0.02)	0.73(0.00)	0.69(−0.02)	0.73(0.02)	0.75(0.03)	0.80(0.02)	4082
1100					0.79(−0.04)	0.75(−0.04)	0.72(−0.04)	0.75(0.00)	0.76(0.01)	0.81(0.00)	3839
1200						0.79(−0.07)	0.74(−0.07)	0.78(−0.01)	0.77(−0.01)	0.82(−0.01)	3728
1300							0.78(−0.08)	0.77(−0.05)	0.79(−0.01)	0.82(−0.03)	3895
1400								0.80(−0.08)	0.79(−0.05)	0.83(−0.05)	3948
1500									0.82(−0.06)	0.85(−0.05)	4129
1600										0.88(−0.06)	4292
1700											4884

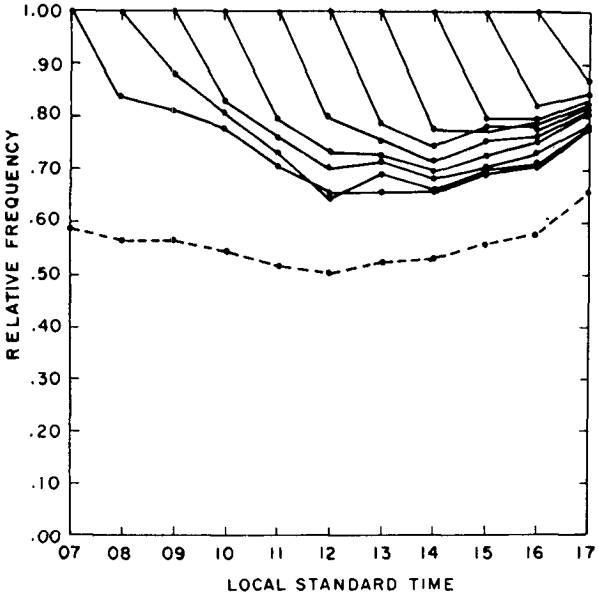

FIG. 10. Relative frequency of recurrence of a cloud-free line-of-sight. The dashed line depicts the unconditional relative frequency of a cloud-free line-of-sight.

data in Table 6 was found with $a=0.383$ when $b=0.620$. The deviations (D) between the observed conditional probabilities (P) and the estimated conditional probabilities ($\hat{P}$), $D=P-\hat{P}$, are shown in parentheses in Table 6. The deviations are generally small.

7. Comparisons between "clear" and cloud-free lines-of-sight

Lund (1966) devoted most of the introduction of his article to defining a "clear" line-of-sight. He stated

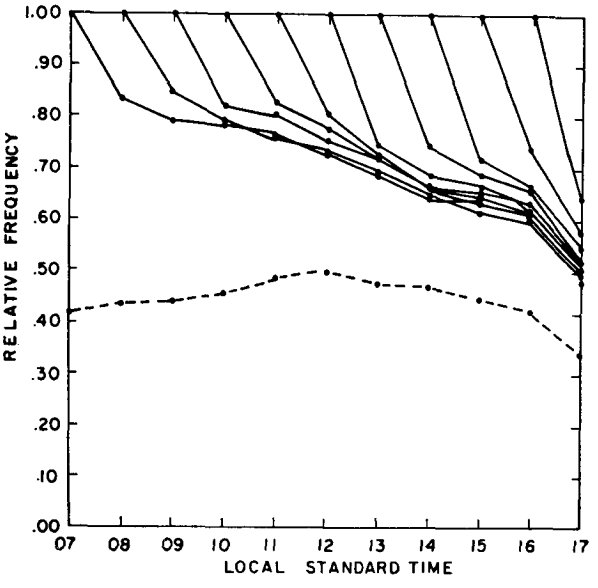

FIG. 11. Relative frequency of recurrence of a cloudy line-of-sight. The dashed line depicts the unconditional relative frequency of a cloudy line-of-sight.

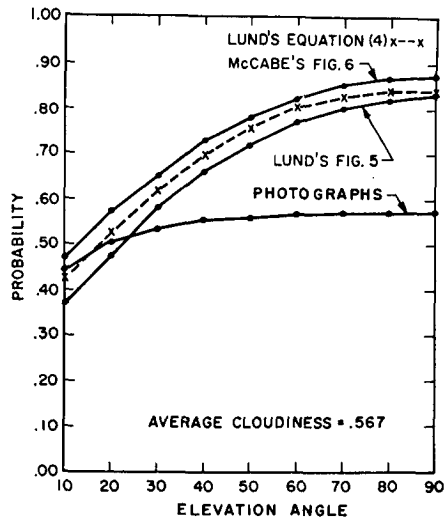

FIG. 12. Probability of a cloud-free line-of-sight as a function of elevation angle as determined from photographs and the probability of a clear line-of-sight as determined from McCabe (1965) and Lund [1966; Eq. (4) and Fig. 6] (see text).

that "A clear line-of-sight is defined as one which permits sufficient bright sunshine (radiation) to pass through the atmosphere to activate the sunshine recorder. Presumably such a condition would also permit sensing a signal through the atmosphere with an optical or infrared detector. The path length is the distance from the top of the atmosphere to the surface of the earth. Since the sunshine recorder does not detect 'thin' clouds, the probability of a clear line-of-sight, as defined in this paper, exceeds the probability of a cloud-free line-of-sight by an amount equal to the probability of 'thin' clouds, roughly 6–20% at the stations under study." In earlier articles by McCabe (1965) and Lund (1965), it is also pointed out that clear does not always mean cloud-free. McCabe (1965) states "It is known that sunshine recorders often record the occurrence of 'bright sunshine' through thin clouds, especially at high sun angles." These statements have been frequently overlooked by users of the graphs and equations developed by McCabe and Lund.

Fig. 12 depicts probabilities of cloud-free lines-of-sight that were determined from hourly photographs taken during four summers at Columbia when the average cloudiness was 0.567. Also shown on Fig. 12 are the probabilities of "clear" lines-of-sight that were estimated from Lund's (1966) Eq. (4) and Fig. 5, and McCabe's Fig. 6. The differences in probabilities between "clear" and cloud-free lines-of-sight are small at low angles of view but exceed 25% at the zenith angle.

8. A general method for estimating probabilities of cloud-free lines-of-sight

In private communication, Rapp and Schutz of Rand Corporation, Santa Monica, Calif., proposed ob-

taining estimates of probabilities of cloud-free lines-of-sight through the use of a formula of the form

$$\hat{P}(\alpha)=\sum_{k=0}^{10} C(\alpha|k)P(k), \qquad (2)$$

where $\hat{P}(\alpha)$ is the probability of a cloud-free line-of-sight through the atmosphere at the angle α, $C(\alpha|k)$ is the probability of a cloud-free line-of-sight at angle α given k tenths of cloudiness, and $P(k)$ is the probability of k tenths of cloudiness.

They suggested that the graph prepared by McCabe (1965) might be used to estimate the $C(\alpha|k)$ values. Since McCabe's graph was based on sunshine observations, the estimates are more representative of "clear" line-of-sight probabilities, as defined by McCabe (1965) and Lund (1966), than cloud-free lines-of-sight.

Since Figs. 5 and 7 are based on data obtained from whole-sky photographs, which detect clouds accurately, and National Weather Service observations of tenths of cloudiness, Eq. (2) recovers the desired probabilities exactly for the data used in this study. Limitations in the size of the data sample used to prepare Figs. 5 and 7 result in some irregularities in the probability curves, and it is also possible that some haze overhead is interpreted as clouds. To partially overcome these limitations Figs. 13 and 14 were prepared. They are the result of subjectively smoothing the curves shown in Figs. 5 and 7, respectively. In our judgment Eq. (2) will yield excellent estimates of probabilities of cloud-free lines-of-sight for most locations if $C(\alpha|k)$ values are interpolated from Fig. 13. For locations where a large fraction of the clouds are cumuliform, for example in the tropics, it may be better to use Fig. 14 rather than Fig. 13 when estimating $C(\alpha|k)$ values.

As an example of the use of Eq. (2) let us assume that we wish to estimate the probability $\hat{P}(40)$ of a cloud-free line-of-sight at an elevation angle of 40° at Columbia, Mo. The last column of Table 1 shows the $P(k)$ values to be 0.153, 0.062,..., 0.076 and 0.265 for $k=0$, 1,..., 9 and 10, respectively. From Fig. 13 the $C(40|k)$ values are approximately 1.00, 0.94,..., 0.29 and 0.10 for $k=0$, 1,..., 9 and 10, respectively. According to the formula,

$$\hat{P}(40)=(1.00)(0.153)+(0.94)(0.062)+\cdots+(0.29)(0.076)+(0.10)(0.265)=0.552. \qquad (3)$$

From the data $P(40)=0.556$; this value is rounded to 0.56 at the bottom of Table 1, column 40°.

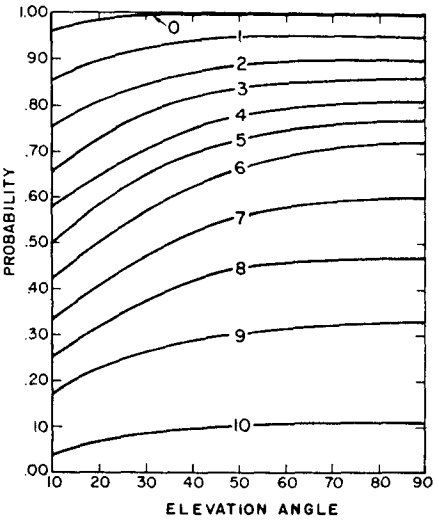

FIG. 13. Probability of a cloud-free line-of-sight as a function of elevation angle and National Weather Service observed total sky cover, in tenths (with smoothing).

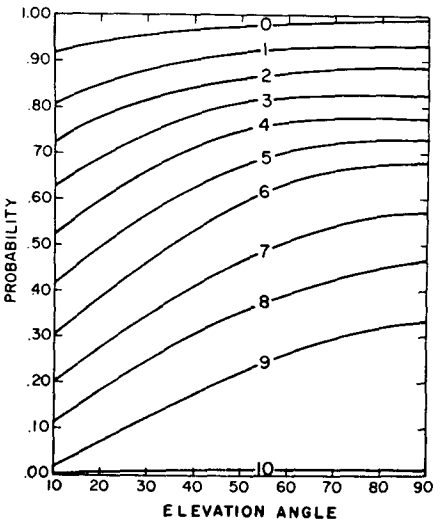

FIG. 14. Probability of a cloud-free line-of-sight as a function of elevation angle and National Weather Service observed total sky cover, in tenths, when one or more of the following cloud types are reported: cumulonimbus, cumulonimbus mammatus, cumulus, fracto-cumulus (cumuliform clouds only) (with smoothing).

9. Conclusions

A climatology derived from whole-sky photographs especially taken to obtain an understanding of problems of seeing through the atmosphere reveals that:

1) Probabilities of cloud-free lines-of-sight through the entire atmosphere between the surface of the earth and space can be accurately estimated from routine observations of total cloud cover through the use of Eq. (2) and values obtained from either Fig. 13, or Fig. 14 (derived from this new climatology based on cloud pictures), depending on the prevalence of cumuliform clouds.

2) Probabilities of recurrence can be accurately estimated from unconditional probabilities of cloud-free lines-of-sight through the use of Eq. (1).

3) For the first three hours, a simple Markov decay model will yield persistence probabilities within a few percent of the median relative frequencies obtained from the data.

4) None of the previously available techniques that use standard weather observations for estimating probabilities of cloud-free lines-of-sight provide accurate estimates. Some of the techniques are intended to yield probabilities of "clear" lines-of-sight under very specific conditions such as a line is clear if sunshine is recorded; others make no provisions for the viewing angle.

10. Remarks

As has been emphasized in the Introduction and Conclusions, this study pertains to seeing through the entire atmosphere. Only the collection of in-flight line-of-sight observations along specific angles (such as the current U. S. Air Force program assisted by the U. S. Navy, Royal Air Force and some commercial airlines) will provide data for estimating probabilities of clear, clouded, or hazy lines-of-sight between flight levels and the surface; and between flight levels and space. With sufficient observations, accurate probabilities will be obtainable for many practical problems. It is also possible to infer probabilities between levels from climatologies based on such in-flight observations.

Acknowledgments. The authors are grateful to Dr. Larry O. Pochop, University of Wyoming, who was responsible for accumulating much of the data and shared in the development of the photogrammetric method; Dwaine S. Bundy and Joseph B. Landwehr, Research Assistants, University of Missouri, who accumulated and analyzed much of the data; David A. Horner, Meteorologist in Charge, U. S. National Weather Service, Columbia, Mo., who cooperated fully in the installation of the photographic equipment and in furnishing Weather Bureau data; Eugene A. Bertoni, Air Force Cambridge Research Laboratories, who monitored Air Force Contract No. F19628-68-C-0140 under which the data were collected; and Donald J. Armstrong and James F. Atkinson, Analysis and Computer Systems, Inc., who provided expert computational support.

REFERENCES

Appleman, H. S., 1962: A comparison of simultaneous aircraft and surface cloud observations. *J. Appl. Meteor.*, **1**, 548–551.

Bertoni, E. A., 1967: Clear lines-of-sight from aircraft. Air Force surveys in Geophysics, No. 196, Air Force Cambridge Research Laboratories, Bedford, Mass., 181 pp.

Blackmer, R. H., Jr., and J. Harllee, 1960: Determination of the per cent of time the ground is visible from an aircraft flying above clouds. Sci. Rept. No. 1, Contract AF 19(628)-7312, Stanford Research Institute, Calif., 30 pp.

Brintzenhofe, R. A., J. L. Cox, J. T. Williams and C. J. Neumann, 1971: Probability of a clear line-of-sight through the atmosphere for a satellite-based laser communications system: A feasibility study. NOAA Tech. Memo. NWS SOS-7, 36 pp. National Technical Information Service, Springfield, Va.

Bundy, D. S., 1969: A two year study of the probability of cloud-free lines-of-sight at Columbia, Missouri. M.S. dissertation, University of Missouri, Columbia, 121 pp.

Eastman Kodak, 1959: Infrared and ultraviolet photography. Kodak Publications No. M-3, 6th ed., 55 pp.

Ehrenreich Photo Optical Industries, Inc., 1965: Fish-eye Nikkor Manual. Tokyo, Japan, 14 pp.

Fox, R. L., 1961: Sunshine-cloudiness relationships in the United States. *Mon. Wea. Rev.*, **89**, 543–548.

Gringorten, I. I., 1971: Modelling conditional probabilities. *J. Appl. Meteor.*, **10**, 646–657.

Lund, I. A., 1965: Estimating the probability of a clear line-of-sight from sunshine and cloud cover observations. *J. Appl. Meteor.*, **4**, 714–722.

——, 1966: Methods for estimating the probability of clear lines-of-sight, or sunshine, through the atmosphere. *J. Appl. Meteor.*, **5**, 625–630.

McAllister, C. R., 1969: Cloud-cover recurrence and diurnal variation. *J. Appl. Meteor.*, **8**, 769–777.

McCabe, J. T., 1965: Estimating mean cloud and climatological probability of cloud-free lines-of-sight. Tech. Rept. 186, Environmental Technical Applications Center, USAF, Navy Yard Annex, Washington D. C., 26 pp.

Pochop, L. O., and M. D. Shanklin, 1966: Sky cover photograms, a new technique. *Weatherwise*, **19**, 198–200.

Shanklin, M. D., and J. B. Landwehr, 1971: Photogrammetrically determined cloud-free lines-of-sight at Columbia, Missouri. Final Report, Contract No. F19628-68-C-0140, Air Force Cambridge Research Laboratories, Bedford, Mass., 185 pp.